

Discriminating fingerprints of chronic neuropathic pain following spinal cord injury using artificial neural networks and mass spectrometry analysis of female mice serum

Meritxell Deulofeu^{a,b,c}, Eladia M. Peña-Méndez^d, Petr Vaňhara^{c,e}, Josef Havel^b, Lukáš Morán^{c,f}, Lukáš Pečinka^{b,e}, Anna Bagó-Mas^a, Enrique Verdú^a, Victoria Salvadó^{g,**}, Pere Boadas-Vaello^{a,*}

^a Research Group of Clinical Anatomy, Embryology and Neuroscience (NEOMA), Department of Medical Sciences, University of Girona, Girona, Catalonia, Spain

^b Department of Chemistry, Faculty of Science, Masaryk University, Kamenice 5/A14, 625 00, Brno, Czech Republic

^c Department of Histology and Embryology, Faculty of Medicine, Masaryk University, 62500, Brno, Czech Republic

^d Department of Chemistry, Analytical Chemistry Division, Faculty of Sciences, University of La Laguna, 38204 San Cristóbal de La Laguna, Tenerife, Spain

^e International Clinical Research Center, St. Anne's University Hospital, 656 91, Brno, Czech Republic

^f Research Centre for Applied Molecular Oncology (RECAMO), Masaryk Memorial Cancer Institute, Brno, Czech Republic

^g Department of Chemistry, Faculty of Science, University of Girona, 17071, Girona, Catalonia, Spain

ARTICLE INFO

Keywords:

Central neuropathic pain
spinal cord injury
mass spectrometry
Artificial intelligence
Artificial neural networks
MALDI-TOF MS
Spectral profiles

ABSTRACT

Spinal cord injury (SCI) often leads to central neuropathic pain, a condition associated with significant morbidity and is challenging in terms of the clinical management. Despite extensive efforts, identifying effective biomarkers for neuropathic pain remains elusive. Here we propose a novel approach combining matrix-assisted laser desorption/ionization time-of-flight mass spectrometry (MALDI-TOF MS) with artificial neural networks (ANNs) to discriminate between mass spectral profiles associated with chronic neuropathic pain induced by SCI in female mice. Functional evaluations revealed persistent chronic neuropathic pain following mild SCI as well as minor locomotor disruptions, confirming the value of collecting serum samples. Mass spectra analysis revealed distinct profiles between chronic SCI and sham controls. On applying ANNs, 100% success was achieved in distinguishing between the two groups through the intensities of m/z peaks. Additionally, the ANNs also successfully discriminated between chronic and acute SCI phases. When reflexive pain response data was integrated with mass spectra, there was no improvement in the classification. These findings offer insights into neuropathic pain pathophysiology and underscore the potential of MALDI-TOF MS coupled with ANNs as a diagnostic tool for chronic neuropathic pain, potentially guiding attempts to discover biomarkers and develop treatments.

1. Introduction

In addition to causing motor dysfunction, spinal cord injury (SCI) can also lead to the development of neuropathic pain (NP) (Ahuja et al., 2017; Burke et al., 2017). The prevalence of NP following SCI may affect up to 80% of patients (Ahuja et al., 2017; Burke et al., 2017; Cardenas and Felix, 2009; Hunt et al., 2021), significantly impacting their quality of life (Failde et al., 2018; Rivers et al., 2018; Vall et al., 2006). NP is characterized not only by reflexive pain responses but also by comorbid mood disorders (Murray et al., 2007; Rivers et al., 2018;

Saurí et al., 2017), posing considerable challenges in medical management. Epidemiological data suggests that women have a heightened vulnerability to the development of emotional comorbid pain disorders (Goesling et al., 2013; Miller and Cano, 2009), highlighting the importance of including female sex as a criterion in the design of chronic pathological pain research studies.

SCI-induced neuropathic pain is a subtype of pathological pain, which is maladaptive rather than protective, resulting from the abnormal functioning of the nervous system after injury (Treede et al., 2019). The high prevalence of pathological pain, including neuropathic

* Corresponding author.

** Corresponding author.

E-mail addresses: victoria.salvado@udg.edu (V. Salvadó), pere.boadas@udg.edu (P. Boadas-Vaello).

<https://doi.org/10.1016/j.neuint.2024.105890>

Received 9 May 2024; Received in revised form 21 October 2024; Accepted 22 October 2024

Available online 23 October 2024

0197-0186/© 2025 The Authors. Published by Elsevier Ltd. This is an open access article under the CC BY license (<http://creativecommons.org/licenses/by/4.0/>).

pain, can be attributed partly to the limited efficacy of available treatments, since those used for neuropathic pain management often have only modest benefits and restricted to a minority of cases (Attal, 2019; Cohen and Mao, 2014; Pirvulescu et al., 2022). This longstanding inefficacy primarily stems from the challenge of precisely targeting underlying mechanisms (Cohen and Mao, 2014). This knowledge gap illustrates the unmet need for identifying specific biomarkers for pathological pain and without a gold standard for diagnosis or treatment, this health condition remains challenging to address, contributing to its chronicity and worsening patients' quality of life (Morlion et al., 2018). In this context, the pursuit of pain biomarkers for diagnostic purposes has emerged as a significant challenge (Chae et al., 2022). Despite extensive directed efforts to identify specific biomarkers for various pathological pain conditions, neither the Food and Drug Administration in the USA nor the European Medicines Agency has yet validated any biomarkers for chronic pain (Smith et al., 2017).

The use of proteome and metabolome for biomarker discovery, facilitated by advanced analytical techniques such as mass spectrometry, as a method of understanding complex diseases such as pathological pain has not given positive results to date (Duncan et al., 2016). In this paper we propose an alternative non-targeted approach that analyses the entire proteome or metabolome without focusing on specific compounds. This approach has been demonstrated to be valuable for generating hypotheses and detecting differences between healthy and diseased samples (Deulofeu et al., 2021; Liu and Locasale, 2017; Schrimpe-Rutledge et al., 2016). In fact, single biomarkers may not be sufficient for clinical diagnosis, prompting the need for fingerprinting or profiling techniques that identify patterns of multiple proteins (Bäckryd et al., 2015; Duncan et al., 2016) that will offer both insights into disease mechanisms and identify potential treatment targets. In line with this approach, we recently developed an innovative, simple, and fast method for detecting and classifying pathological pain subtypes in experimental models using serum mass spectra (Deulofeu et al., 2023). Specifically, the analysis of pain response outcomes and MALDI-TOF MS serum spectra, in combination with artificial neural network (ANN) analyses, provides a methodology for identifying neuropathic and nociplastic pain subtypes and determining their origin through their fingerprints, without the need to identify single biomarkers (Deulofeu et al., 2023). However, this methodology was developed with acute pathological pain models, and to the best of our knowledge, there are no studies focused on fingerprinting discrimination of SCI-induced chronic neuropathic pain. It is worth mentioning that traumatic SCI in humans is pathophysiologically categorized into primary and secondary injuries, with temporal distinctions including acute (<48 h), subacute (48 h–14 days), intermediate (14 days–6 months), and chronic (>6 months) phases (Norenberg et al., 2004). Considering the dynamic nature of these processes, the array of molecules involved in each phase may vary, suggesting that it might be possible to use overall molecular profiles to differentiate between phases. Consequently, while the fingerprinting of acute SCI has already been established (Deulofeu et al., 2023), it would be valuable to determine the specific profiles associated with chronic SCI.

In light of the above considerations, this study aims to evaluate the effectiveness of combining MALDI TOF MS with ANN analysis to classify mass spectral profiles associated with chronic neuropathic pain induced by SCI in female mice. This approach holds promise as a clinical decision support tool for diagnosing and monitoring chronic pain, and it could lay the groundwork for future investigations into multiple biomarkers for chronic neuropathic pain, potentially leading to the development of more targeted treatments.

2. Materials and methods

2.1. Animals

Adult female ICR-CD1 mice (20–30 g) were procured from Janvier

Laboratories (France). The use of mice was minimized with experimental groups comprising 14–15 mice each. The determination of the animal sample size required for functional evaluation was conducted using GRANMO (Version 7. April 12, 2012), ensuring adherence to the ethical guidelines established by the Animal Ethics Committee of the University of Barcelona. Mice were housed in standard plexiglass cages (28 × 28 × 15 cm) with unrestricted access to food and water, maintained under a 12:12 h light/dark cycle, at a temperature of 21 ± 1 °C, and humidity levels ranging from 40% to 60%. Cage cleaning occurred twice weekly. All mice underwent a minimum 1-h acclimatization period to the facility rooms before engaging in any functional or surgical procedures, all of which were conducted during the light cycle. Regular testing of sentinel mice ensured the absence of pathogens throughout the experimental period.

All procedures performed on animals and their care adhered to the ARRIVE 2.0 guidelines and complied with the ethical principles outlined by the International Association for the Study of Pain (I.A.S.P.) for assessing pain in conscious animals (Zimmermann, 1983), as detailed in the European Parliament and Council Directive of September 22, 2010 (2010/63/EU). The study protocol received approval from both the Animal Ethics Committee of the University of Barcelona and the Government of Catalonia (DAAM number 8884).

2.2. Experimental design and surgical procedure

Female CD-1 WT mice were submitted to a mild SCI and data on reflexive pain responses (thermal hyperalgesia and mechanical allodynia) were collected using the von Frey test and plantar test, respectively, from the acute phase through to the chronic phase (0, 1, 2, 3, 6, 9, and 12 weeks post-injury). With regard to the surgery, following anesthesia, spinal cord contusion was induced using a weight-drop device as detailed elsewhere (Castany et al., 2023; Soler-Martínez et al., 2022), ensuring the induction of central neuropathic pain without inducing paralysis in the animals. After a dorsal laminectomy, the T8–T9 thoracic spinal cord segments were exposed, and a weight of 2 g was dropped from a height of 25 mm onto a metallic stage positioned over the exposed spinal cord (SCI group). Post-procedure, the wound was closed, and the animals were kept in a warm environment until full recovery. Additionally, animals received 0.5 mL of saline solution to replenish any potential blood volume deficit. As controls, a sham group of mice, in which the spinal cord was exposed but not subjected to contusion, was used. At the end of the experimental period, serum samples were collected and processed for further acquisition of mass spectra by MALDI TOF. Subsequently, data obtained from mass spectral profiles and functional evaluation procedures were used to determine whether combining MALDI TOF MS with ANN analysis could serve as an effective methodology for classifying mass spectral profiles associated with chronic neuropathic pain induced by SCI.

2.3. Reflexive pain response evaluation

Thermal hyperalgesia was evaluated by recording hind paw withdrawal latency in response to radiant heat applied with the plantar test apparatus (#37370; Ugo Basile, Comerio, Italy) as previously described (Bagó-Mas et al., 2022; Deulofeu et al., 2023). Mice were allowed to acclimate on the tempered (29 °C) glass surface of the exploratory plantar cage. The radiant heat source was positioned under the plantar surface of the hind paw, with a time-limit of 25 s to avoid skin damage. Withdrawal latencies for both hind paws were determined from the average of three separate trials conducted at 5-min intervals. Both paws were evaluated given that the SCI model results in bilateral injury.

In the case of mechanical allodynia, quantification involved the assessment of 50% withdrawal thresholds using a series of von Frey monofilaments (bending force range: 0.04–2 g) following the up-down paradigm, as described previously (Bagó-Mas et al., 2022; Deulofeu et al., 2023). Each filament was applied to the plantar surface of the

mice for 2 s, with a progressively thicker filament being employed until a nociceptive response was observed after which a thinner filament was applied. Four measurements were taken using this procedure and both hind paws were tested and averaged. A 50% response rate was calculated using the Dixon formula (Dixon, 1980): 50% paw withdrawal threshold (g) = $[(10(Xf + \kappa\delta)/10,000)]$, where Xf represents the value (in logarithmic units) of the final von Frey filament used, κ is a fixed tabular value for the pattern of positive/negative responses, and δ is the mean difference (in log units) between stimuli.

Finally, the locomotor activity was assessed using the Basso Mouse Scale (BMS) test (Basso et al., 2006), performed as described elsewhere (Bagó-Mas et al., 2022; Castany et al., 2023). In brief, animals were individually placed in a circular plastic open field (70 cm diameter x 24 cm wall height) and given 5 min to move freely. During this time, hindlimb movements were assessed based on stepping, paw position, coordination, and trunk stability (the BMS score ranges from 0 (no hindlimb movement) to 9 (normal, coordinated gait)).

2.4. Sample collection and acquisition of mass spectra

Upon completion of the experimental protocol, all animals were anesthetized with sodium pentobarbital (90 mg/kg; i.p.) and blood collection was performed via the insertion of an intracardiac needle. The collected blood was subsequently centrifuged for 15 min at 4000 rpm to obtain serum, which was promptly frozen in dry ice and stored at -80°C until analysis by MALDI-TOF MS.

For MS analysis, a previously optimized protocol was employed (Deulofeu et al., 2023). Briefly, serum samples (maximum 10 μL) were initially diluted tenfold with double distilled water (dd-H₂O) and mixed in a 1:1 ratio with a sinapinic acid (SA) solution containing 20 mg SA/mL in 60%:40% (v/v) acetonitrile (ACN): dd-H₂O with 0.3% trifluoroacetic acid (TFA) to enhance ionization. Subsequently, 1 μL of the mixture was applied in triplicate to a purified stainless-steel target plate (Basheer and Hajmeer, 2000; Deulofeu et al., 2023). Mass spectra were then obtained using a MALDI-7090 TOF mass spectrometer (Kratos Analytical Ltd., UK), which was equipped with 2 kHz ultra-fast solid-state UV laser (Nd-YAG:355 nm), delayed extraction, and a micro-channel plate detector. The laser energy was expressed in arbitrary units (a.u.) and set at 140 a.u., with a laser fluence of approximately 10 mJ/mm²/pulse. The accelerating voltage was maintained at 20 kV, and laser repetition occurred at 5 Hz with a pulse time width of 3 ns. All measurements were conducted in positive linear mode, and the mass range analyzed ranged from 0 to 10,000 Da. The automatic mode was configured to record all mass spectra using a regular raster, with the spectra registered as the relative ion signal to the mass-to-charge (m/z) value. Normalization of the spectra was performed with the maximum peak intensity set to 100%. Additionally, matrix samples served as blanks and were analyzed to distinguish matrix peaks from those of the samples. Solutions software (Kratos Analytical Ltd.) was used for to evaluate and export the mass spectra.

2.5. Statistical analysis and artificial neural networks

Functional assessments (reflexive pain responses) were performed in a blinded manner, with each mouse assigned an identification code. To determine the appropriate statistical tests, data normality was first evaluated using the Kolmogorov-Smirnov test. Based on this assessment, either parametric or non-parametric methods were applied. For normally distributed data, repeated measures MANOVA (Wilks' criterion) and ANOVA were utilized, followed by Duncan's post-hoc test where necessary. In cases where data did not meet normality assumptions, the Friedman test for non-parametric repeated measures and the Kruskal-Wallis test, followed by the Mann-Whitney U test, were used. A significance level of $\alpha = 0.05$ was applied to all statistical tests, which were conducted using SPSS version 25.0 for Windows. Results are expressed as mean \pm standard deviation of the mean (SEM).

As for ANNs, they serve as a mathematical model inspired by human neural architecture, aiming to mimic the brain's ability for learning and generalization. They excel in modeling non-linear systems where relationships among variables are intricate or even unknown, while remaining resilient to signal-to-noise interference (Agatonovic-Kustrin and Beresford, 2000; Basheer and Hajmeer, 2000). Consequently, ANNs prove adept at pattern recognition and classification, making them valuable tools for clinical diagnosis (Agatonovic-Kustrin and Beresford, 2000; Amato et al., 2013; Basheer and Hajmeer, 2000; Deulofeu et al., 2019; Houska et al., 2014). ANN analyses were performed as described elsewhere (Deulofeu et al., 2023). Following the exportation of mass spectra, the data underwent preprocessing using R Studio software. This involved several steps: background removal, signal intensity normalization, smoothing, and baseline subtraction using the Savitzky-Golay and Loess methods along with spectral alignment. The objective of this preprocessing was to minimize variance within databases (Norris et al., 2007). Mass spectra were analyzed individually to construct databases of chronic SCI and chronic Sham models. Additionally, another database was created to compare spectral fingerprints across the chronic and acute models. Before commencing statistical analyses, the resulting files containing mass spectra information, including non-relevant data, were reviewed and cleaned. Only peaks with a variance (s^2) greater than 1 were retained in the final database after calculating the variance of the mean intensity of different peaks. Z-scaling was then applied to each dataset, and principal component analysis (PCA) was performed using the SPSS 25.0 statistical package. The main m/z variables and functional data were selected to construct PCAs using TRAJAN 3 software, facilitating model classification. A multilayer perceptron network, comprising artificial neurons organized in input, hidden, and output layers, was employed for all experiments. The architecture of this ANN was optimized with the number of nodes in the hidden layer chosen to minimize the root mean squared error. In all experiments, an architecture with three nodes in the hidden layer was used. The inputs of the networks were the intensities of selected m/z signals that were specific to each model. The network was trained using the back-propagation algorithm with a maximum of 50,000 iterations and a classification confidence level of 0.05. After the training phase, the model's performance was assessed using leave-one-out cross-validation to evaluate its predictive capability in classifying single samples excluded from the training dataset. Cases not identified by the ANN were classified as erroneous predictions.

3. Results

3.1. Chronic neuropathic pain persists following mild spinal cord injury with only minor disruptions to locomotor abilities

Prior to conducting MALDI-TOF MS serum analysis, the two experimental groups of animals, sham_C (n = 14) and SCI_C (n = 14), underwent evaluation to determine the progression of reflexive pain responses, thermal hyperalgesia and mechanical allodynia throughout the chronic phase of SCI (up to 12 weeks post-injury).

The thermal hyperalgesia data exhibited a normal distribution ($p > 0.5$), based on the Shapiro-Wilk test. MANOVA analysis revealed significant effects attributed to the week ($p < 0.01$), injury ($p < 0.001$), and the interaction between the factors of week and injury ($p < 0.01$). Further ANOVA analysis indicated significant group differences at all assessment time-points post-lesion (weeks 1–6 and 12, $p < 0.001$; week 9, $p < 0.01$). Throughout the post-injury period, spinal cord injured mice demonstrated decreased paw withdrawal latency to thermal stimulation compared to the sham group (Fig. 1A).

In terms of mechanical allodynia data, the Shapiro-Wilk test revealed a non-normal distribution. Consequently, non-parametric Friedman and Mann-Whitney U tests were employed for statistical analysis. The Friedman test for variance analysis indicated that data distribution varied across the experimental period. Subsequent Mann-Whitney U

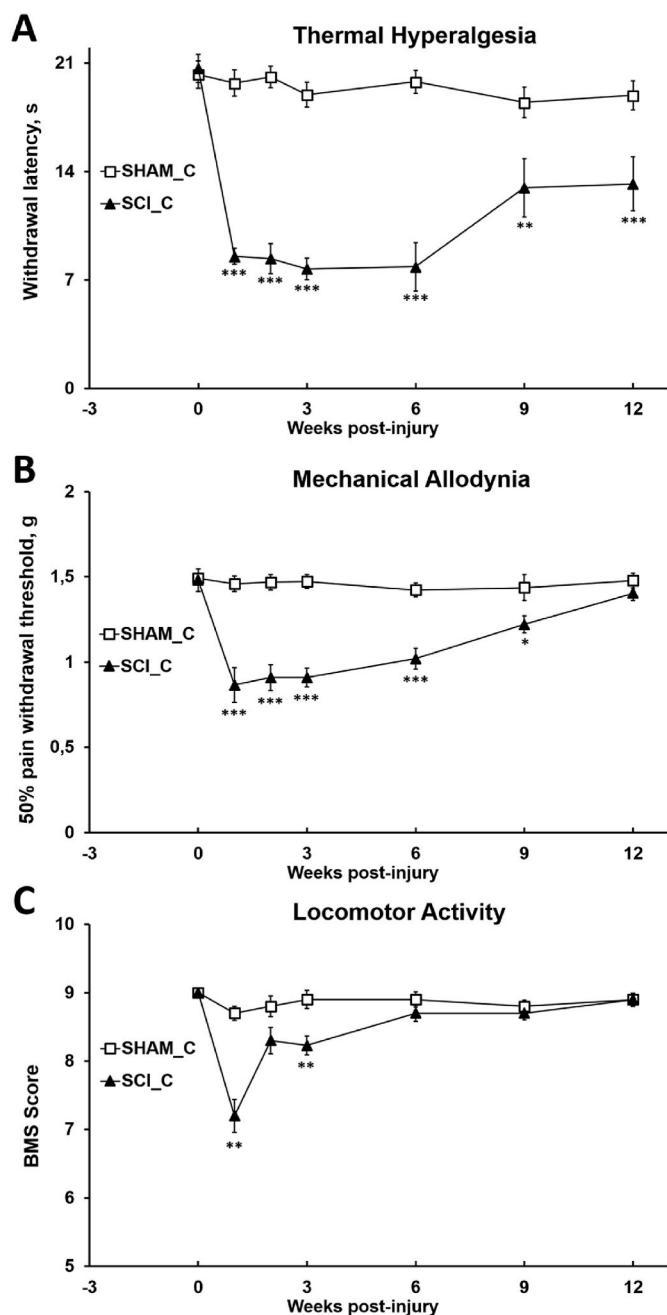


Fig. 1. Time-course assessment of thermal hyperalgesia, mechanical allodynia, and locomotor activity following mild spinal cord injury during the chronic phase. Mean values along with standard error of the mean (SEM) are depicted using points and vertical lines. Two experimental groups were compared: sham_C (n = 14) and SCI_C (n = 14). (A) Thermal hyperalgesia was significantly observed in SCI animals for up to 12 weeks post-injury (wpi), with data analyzed via unidirectional ANOVA. (B) Mechanical allodynia was also significantly present in SCI animals up to 9 wpi, analyzed using the Mann-Whitney non-parametric test. (C) Mild alterations in BMS were noted, indicating changes in paw position without affecting horizontal locomotion, but were only present in weeks 1 and 3 post-injury (significance denoted as * $p < 0.05$, ** $p < 0.01$, *** $p < 0.001$).

tests revealed significant intergroup differences from the first to the eighth week post-injury (weeks 1–6, $p < 0.001$; week 9, $p < 0.05$). SCI mice exhibited a decrease in the paw withdrawal threshold to mechanical stimulation from the first to the eighth week post-injury, followed by a subsequent recovery of the withdrawal threshold until the experiment's conclusion, reaching values that were similar to those

observed in the sham group (Fig. 1B).

With regards to locomotor activity, the Shapiro-Wilk test also demonstrated a non-normal distribution ($p < 0.001$). Friedman's test further indicated significant variability in sample distribution throughout the experiment ($p < 0.001$), with the Mann-Whitney U test revealing significant group differences only at post-injury weeks 1 and 3 ($p < 0.01$) (Fig. 1C). Importantly, no major alterations in horizontal locomotion were observed, indicating that all mice retained the ability to move freely without experiencing paralysis or significant impairment in coordination and locomotor functions.

According to defined criteria in the animal welfare protocol (Morton and Griffiths, 1985), all mice exhibited normal characteristics throughout the study period. There were no observed changes in coat or skin condition, vibrissae of the nose, nasal secretions, signs of autotomy, and weight fluctuations, nor were there displays of aggressiveness, allowing us to infer that the functional data obtained were not influenced by any discomfort experienced by the animals.

Overall, these findings indicate that SCI-animals had developed significant chronic central neuropathic pain 12 weeks post-injury and so we can be sure that the subsequently collected serum samples corresponded to mice that were expressing chronic neuropathic pain during the chronic phase of SCI.

3.2. Mass spectrometry data provides information that could enable the distinction between animals suffering from SCI-induced chronic pathological pain and their corresponding controls

After conducting functional *in vivo* experiments, triplicate serum samples obtained from both spinal cord injured mice (SCI_C mice) and sham controls (Sham_C) were analyzed using a MALDI-7090 TOF mass spectrometer. The resulting mass spectra were evaluated to distinguish between pathological samples and their respective control counterparts.

Firstly, in the visual examination of the serum mass spectra, different m/z regions containing multiple peaks with varying signal intensities between the Sham_C and SCI_C groups were detected. Despite this, the mass spectra profiles collected in the positive mode of both SCI_C mice and Sham_C control mice had similar profiles (Fig. 2) and there was no indication that any individual peaks might serve as a group marker.

A more comprehensive examination of the mass spectra was then conducted, resulting in a substantial volume of data encompassing numerous m/z signals in both experimental groups. Following the database preparation outlined in the methodology section, a total of 322 m/z values whose intensity signals had signal-to-noise ratio (s/n) ≥ 3 (according to the IUPAC rules) were first included in the database. Afterwards, the database was cleaned of non-relevant information involving serum signals with variances (s^2) < 1 and matrix m/z values, leaving only intensity signals of 113 m/z values. The univariate box-plot analysis showed that there was significant variability between the intensities of 12 of the selected m/z values of the mass spectra of both groups (Fig. 3A). These datasets underwent PCA to unveil potential distinct metabolomic patterns associated with SCI_C mice. Subsequently, the samples were plotted based on the three first principal components (PCs) on a 3D score plot, enhancing visualization and facilitating the identification of trends and outliers in data (Deulofeu et al., 2023; Monakhova and Goryacheva, 2016). Despite the overlap, the resulting plot clearly delineated two clusters (Fig. 3B).

Taken together, these findings indicate that most of the SCI_C serum mass spectrum data can be clearly differentiated from their respective Sham_C controls, suggesting the potential presence of metabolomic patterns within these mass spectra that may be analyzed by ANN to develop a classification method.

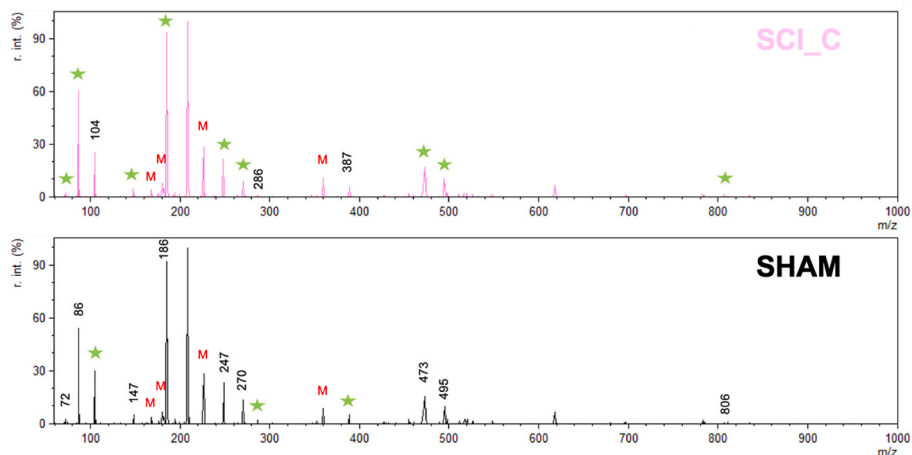


Fig. 2. Representative serum mass spectra from both chronic SCI and chronic sham mice were obtained using MALDI-TOF MS during the chronic phase of the injury. Observable differences between the SCI_C and Sham_C groups are evident. Stars are used to indicate the signals with the highest intensities of certain m/z values.

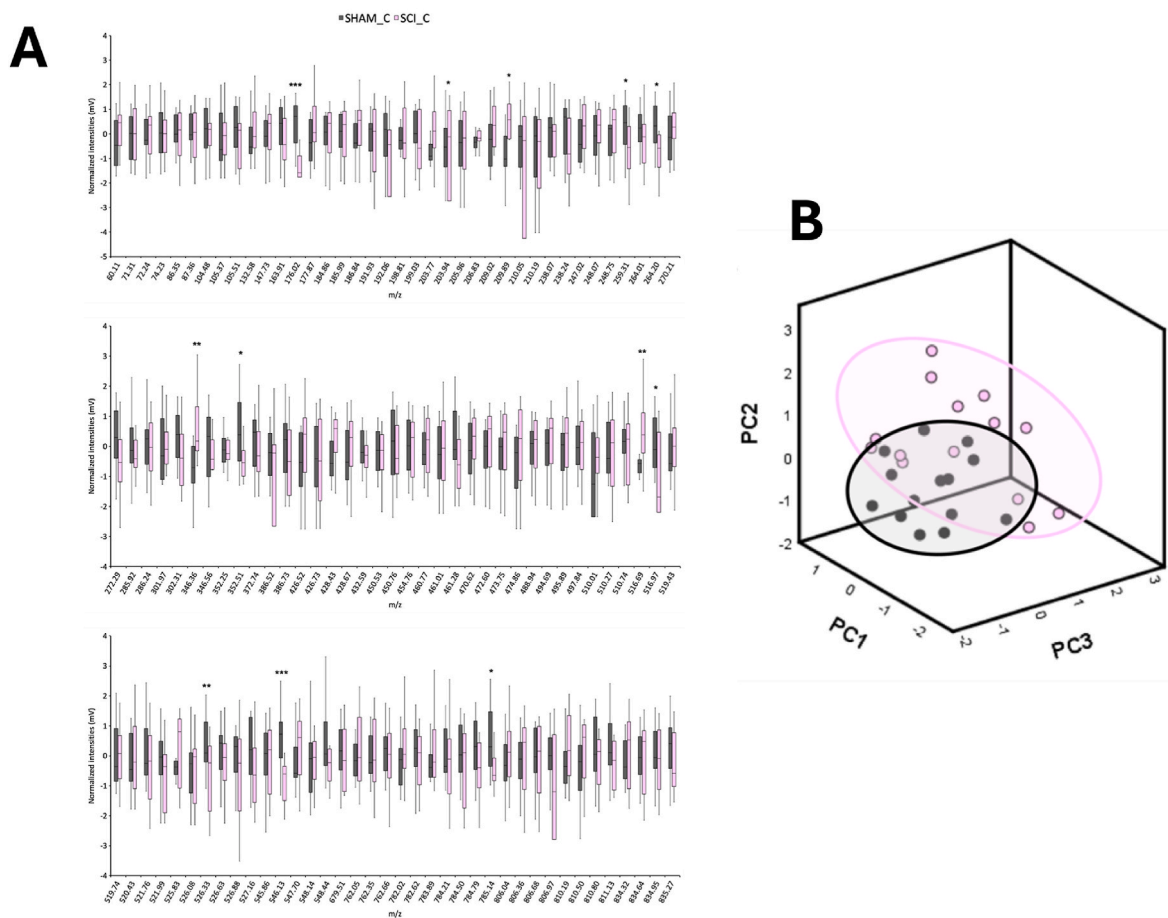


Fig. 3. (A) Intensities of the most relevant m/z peaks found in the serum analysis by MALDI-TOF MS Data shown as the median of each group \pm interquartile range (IQR) (* $p < 0.05$, ** $p < 0.01$, *** $p < 0.001$); (B) PCA statistical analysis using 113 peaks (m/z values) of mass spectrum data obtained from the spinal cord injury model in the chronic phase of the injury. Experimental groups: Sham_C (n = 14) and SCI_C (n = 14), serum samples of each animal were analyzed by triplicate.

3.3. Serum spectrum profile analysis using ANNs distinguish between samples of SCI-induced chronic pathological pain mice and their corresponding chronic sham controls

A data set consisting of the intensity signals of 113 m/z was employed in the training and verification steps of the ANN analysis

performed with an optimized ANN architecture (113:3:1) with 113 inputs (the 113 m/z values), 3 nodes in the hidden layer and 1 output (sham or SCI group). The optimal number of nodes was found after plotting the root mean square error (RMS) as a function of the number of nodes in the hidden layer (Fig. 4A and B). To train the ANN, more than 50,000 training cycles (epochs) were performed without overfitting the

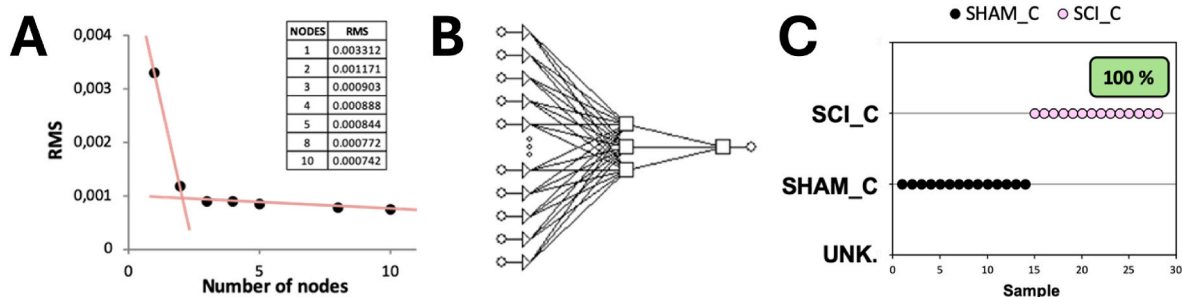


Fig. 4. Serum spectral profile analyses by ANNs of 113 peak database. (A) Plot of the RMS against the number of nodes in the hidden layer corresponding to the analysis using 113 inputs; (B) General architecture of the ANN with 3 nodes in the hidden layer used for discrimination of spectral profiles; (C) Detail of the ANN classification output based on the 113 m/z values. Experimental groups: Sham_C (n = 14) and SCI_C (n = 14).

system, demonstrating the robustness of the model. For the model verification, the leave-one-out cross validation method was performed, achieving a classification success rate of 100% (Fig. 4C).

Subsequently, a new data set was generated after eliminating m/z values that made a minimal statistical contribution to the PCs so as to discard potentially irrelevant values for classification. Fifty-three signals remained in the database and were used for a new PCA calculation. Thirteen PCs (eigenvalues ≥ 0.5), accounting for 97% of the data variability, were derived from this calculation. The subsequent score plot of the samples revealed two groups with a substantial overlapping region between them (Fig. 5A). Upon further ANN analysis using the final 13 PCs, only two samples (one from each group) could not be classified correctly, indicating a 93% correct classification rate (Fig. 5B), which is slightly lower than the success rate obtained using the full database (Fig. 4C). For the ANN analysis, a network architecture featuring three nodes in the hidden layer was employed (Fig. 5C), and no instances of model overfitting were detected even after more than 50,000 epochs.

Overall, these findings show that the signals of the 113 m/z peaks extracted from the mass spectra offer valuable information for sample differentiation through ANN analysis, potentially representing the serum spectral profile or fingerprint of the chronic phase of SCI (Table 1).

3.4. The combination of reflexive pain response outcomes with mass spectra data reduces the effectiveness of ANN in successfully classifying pathological pain and healthy samples

Since functional data might enhance or impair ANN classification of pathological pain, data from the final assessment time-points of thermal hyperalgesia and mechanical allodynia were incorporated into the dataset as new variables. Initially, both of these pieces of functional data were added individually, resulting in two databases that combine the signals of the 113 m/z values with one of the pain response variables. Despite the mechanical allodynia data having a variance < 1 , they were

still included. Both databases underwent PCA, yielding fourteen PCs that explained 95% of the data variability in each case. Similar sample score plots were generated, depicting two groups with a considerable overlapping area (Fig. 6A and B). The databases were then subjected to ANN analysis. When either thermal hyperalgesia or mechanical allodynia and mass spectrum data were used as inputs, three nodes were determined to be the optimal number in the hidden layer in both network architectures (Fig. 6C and D). As for the combination of mass spectrum data and thermal hyperalgesia, the ANN achieved correct classification of 79% of the samples, with only three samples from each group remaining unidentified (Fig. 6E). Conversely, when mechanical allodynia data was used, an 89% classification success rate was achieved. Only three samples (two Sham_C and one SCI_C) were classified as unknown (Fig. 6F).

In the final step, both functional variables were concurrently incorporated into the database. Once again, PCA yielded 14 factors, which now accounted for 94% of the data variability. No notable differences were observed in the score plot of the samples compared to the two previous analyses (Fig. 7A). In the ANN analysis, the optimal network structure remained consistent with three nodes in the hidden layer (Fig. 7B). Notably, no instances of model overfitting were detected during the training process. Twenty-four samples were correctly classified into their respective groups, with only four samples (two from each group) remaining unidentified. Consequently, an 86% correct classification rate was achieved using both functional variables in conjunction with the mass spectrum data (Fig. 7C).

Overall, the results suggest that reflexive pain response data did not offer significant information for the classification of samples by ANN.

3.5. The analysis of serum samples by MALDI-TOF MS in combination with ANN analysis is a useful tool to discriminate between chronic and acute central neuropathic pain samples

Once the MALDI-TOF MS and ANN method had been developed to differentiate chronic neuropathic and sham conditions in SCI, we

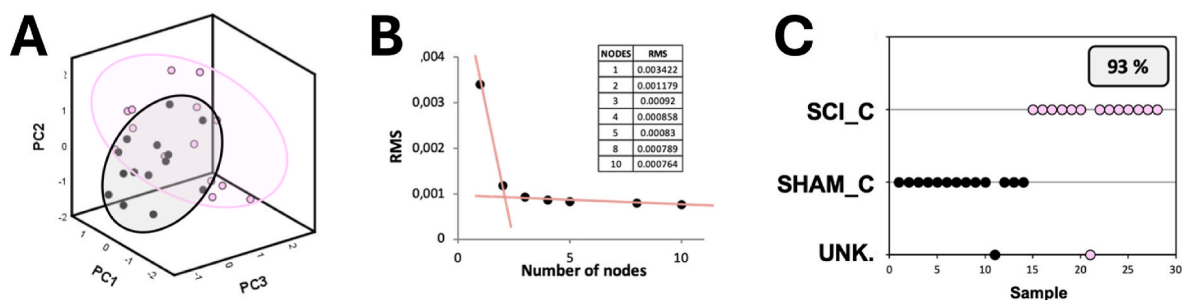


Fig. 5. Serum spectral profile analyses coupling MALDI-TOF MS data and ANN analysis using the intensities of 53 m/z values. (A) PCA using 53 m/z values of mass spectrum data obtained of the SCI model in the chronic phase of the injury; (B) plot of the RMS against the number of nodes in the hidden layer corresponding to the analysis using 53 inputs. Three nodes in the hidden layer were used in the analyses; (C) detail of the ANN classification output based on the 53 m/z values. Experimental groups: Sham_C (n = 14) and SCI_C (n = 14).

Table 1

Serum spectral profile of SCI model in mice during the chronic phase. Relevant peaks used to obtain the best classification success by ANN analysis.

RELEVANT M/Z FOR THE CLASSIFICATION (Da)	
60.11, 70.31, 72.24, 74.23, 86.35, 87.36, 104.48, 105.37, 105.51, 132.58, 147.73, 163.91, 176.02, 177.87, 184.86, 185.99, 186.84, 191.93, 192.06, 198.81, 199.03, 203.77, 203.94, 205.96, 206.83, 209.02, 209.89, 210.05, 210.19, 238.07, 238.24, 247.02, 248.07, 248.75, 259.31, 264.01, 264.20, 270.21, 272.29, 285.92, 286.24, 301.97, 302.31, 236.36, 346.56, 352.25, 372.74, 386.52, 386.73, 426.52, 426.73, 428.43, 428.67, 432.59, 450.53, 450.76, 454.76, 460.77, 461.01, 461.28, 470.62, 472.60, 473.75, 474.86, 488.94, 494.69, 495.89, 497.84, 510.01, 510.27, 510.74, 516.69, 516.97, 519.43, 519.74, 520.43, 521.76, 521.99, 525.83, 526.08, 526.33, 526.63, 526.88, 527.16, 545.86, 546.13, 547.70, 548.14, 548.44, 679.51, 762.05, 762.35, 762.66, 782.02, 782.62, 783.89, 784.21, 784.50, 784.79, 785.14, 806.04, 806.36, 806.68, 806.97, 810.19, 810.50, 810.80, 811.13, 834.32, 834.64, 835.27	

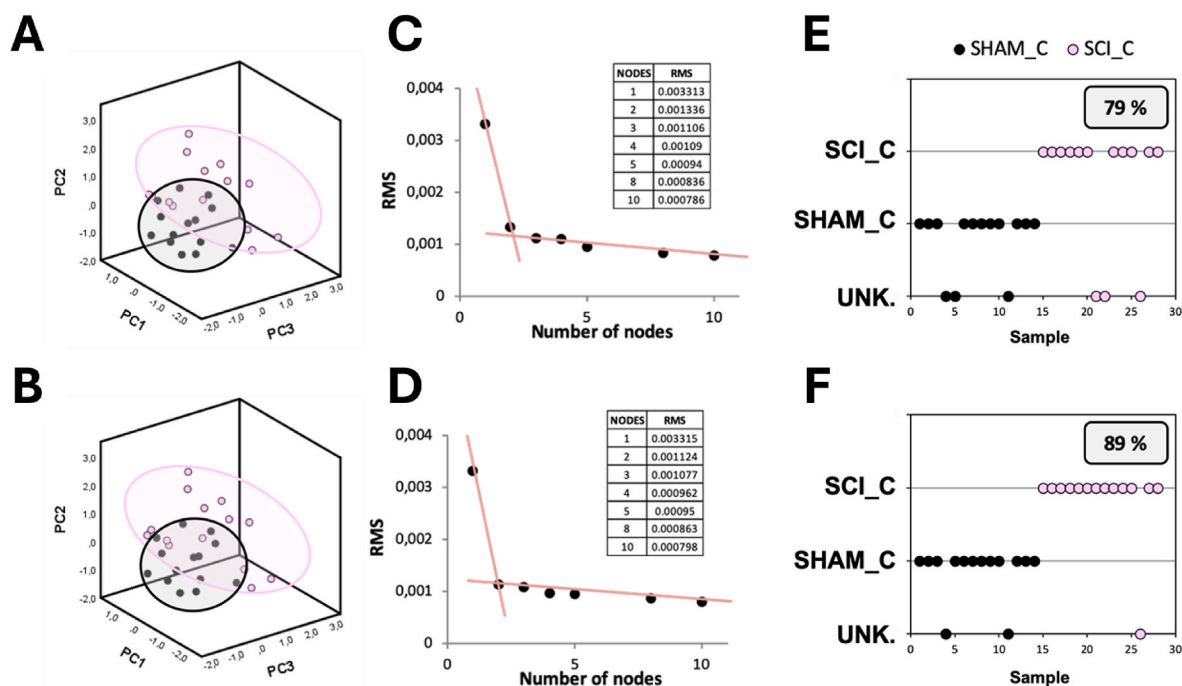


Fig. 6. Serum spectral profile analyses coupling either thermal hyperalgesia or mechanical allodynia outcomes with MALDI-TOF MS data and ANN analysis. (A) PCA results after adding the thermal hyperalgesia outcomes to mass spectrum data; (B) PCA results after adding the mechanical allodynia outcomes to mass spectrum data; (C) plot of the RMS against the number of nodes in the hidden layer corresponding to the analysis using 114 inputs (the signals of 113 m/z values and thermal hyperalgesia data). Three nodes in the hidden layer were used in the analyses; (D) plot of the RMS against the number of nodes in the hidden layer corresponding to the analysis using 114 inputs (the signals of 113 m/z values and mechanical allodynia data). Three nodes in the hidden layer were used in the analyses; (E) detail of the ANN classification output based on the combination of data from mass spectra and thermal hyperalgesia; (F) detail of the ANN classification output based on the combination of data from mass spectra and mechanical allodynia. Experimental groups: Sham_C (n = 14) and SCI_C (n = 14).

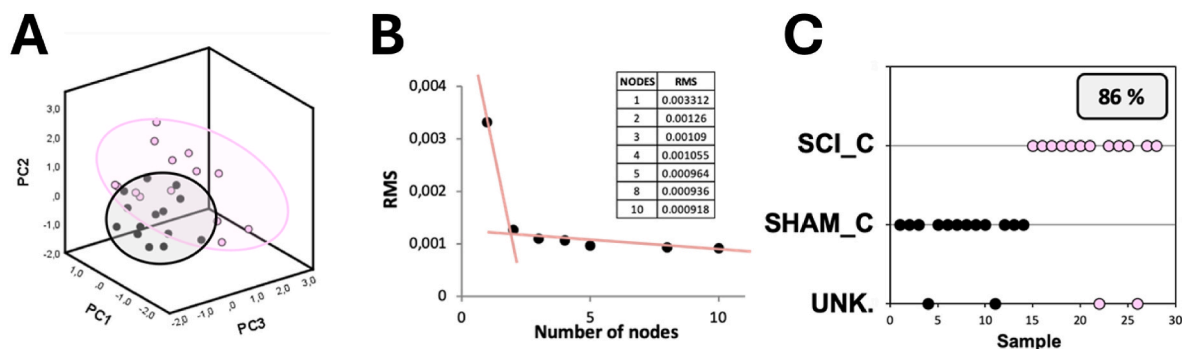


Fig. 7. Serum spectral profile analyses coupling both reflexive pain outcomes, MALDI-TOF MS data and ANN analysis. (A) PCA results after adding both reflexive pain response outcomes to mass spectrum data; (B) Plot of the RMS against the number of nodes in the hidden layer corresponding to the analysis using 115 inputs (the signals of 113 m/z values and both thermal hyperalgesia and mechanical allodynia data). Three nodes in the hidden layer were used in the analyses; (C) detail of the ANN classification output based on the combination of data from mass spectra, thermal hyperalgesia and mechanical allodynia. Experimental groups: Sham_C (n = 14) and SCI_C (n = 14).

focused on testing its ability to detect distinct pain profiles across injury stages. Serum from SCI_C was analyzed alongside samples from mice sacrificed three weeks post-injury (acute phase) in previous experiments

(Deulofeu et al., 2023) to determine if the method could distinguish between the acute and chronic phases. When samples from acute and chronic SCI phases were evaluated together, distinct disparities were

observed when comparing the serum mass spectra of the SCI_C and SCI_A groups. Notably, all m/z values within the mass spectra of SCI_C mice appeared to exhibit lower intensities than the SCI_A group (Fig. 8). However, the most significant differences were noted within the lower mass range of the spectra, spanning from 100 to 1000 Da, which was already evident in previous studies of acute SCI samples (Deulofeu et al., 2023).

After mass spectra acquisition, the intensity signals corresponding to 151 m/z values with a signal-to-noise ratio (s/n) ≥ 3 were included in the database. As described above, this database was cleaned by removing the peaks of the matrix and those from the serum with an $s^2 < 1$, resulting in a database consisting of 55 m/z values. Subsequent statistical analysis revealed that 44 of the 55 m/z values examined had significant differences, predominantly characterized by lower peak intensities in the serum samples of SCI_C mice compared to those of the SCI_A group (Fig. 9).

The data from the 55 selected m/z peaks was analyzed by PCA, yielding twelve factors (eigenvalues ≥ 0.5) that collectively accounted for 97% of the variability. The resulting score plot showed the samples forming two distinct groups (Fig. 10A), although the SCI_C containing three outliers separated from the main group. Subsequently, the same 55 m/z values were used as inputs for the ANN analysis. Network optimization determined that the optimal number of nodes in the hidden layer was three (Fig. 10B). The model's robustness was validated by the absence of overfitting, even after more than 50,000 epochs during the training process. Finally, using the leave-one-out verification method, all samples were accurately classified into their respective groups, achieving a 100% success rate (Fig. 10C).

As in previous experiments involving SCI_C and Sham_C, we sought to determine whether comparable outcomes could be attained with a reduced set of variables. To this end, we systematically eliminated those m/z values that had minimal impact on the PCs identified in the preceding analysis. After this refinement process, a database comprising 42 variables underwent PCA once again, revealing 10 components (eigenvalues ≥ 0.4) that collectively accounted for 96% of the data variability. The resulting score plot of the samples resembled that obtained in the previous PCA, depicting two distinct groups, although with the SCI_A samples exhibiting greater dispersion (Fig. 10D). For the ANN analysis, a network featuring three nodes in the hidden layer was employed (Fig. 10E), and the training process was conducted without encountering overfitting issues. Identical outcomes were observed in the ANN

analysis, with all samples being effectively classified (Fig. 10F), indicating that irrelevant information for sample classification had been successfully eliminated from the database. No further variables could be eliminated from the analysis, as all the 42 m/z values were deemed to be informative, carrying significant weight in at least one of the previous PCs, and so were regarded as relevant peaks for distinguishing samples from spinal cord injured mice at various phases of the injury (Table 2).

4. Discussion

This study aimed to assess the effectiveness of combining MALDI-TOF MS with ANN analysis to classify mass spectral profiles linked to chronic neuropathic pain caused by SCI in female mice. This combined approach could show potential as a clinical decision support tool for diagnosing and tracking chronic pain and might also serve as a foundation for future research into multiple biomarkers for chronic neuropathic pain, potentially leading to the development of more precise treatments.

To achieve this goal, it was first necessary to collect blood samples from animals with chronic neuropathic pain. CD1 female mice were subjected to SCI, their reflexive pain responses were evaluated weekly, and serum was collected after 12 weeks post-injury. The functional evaluation of the SCI and Sham groups to determine the progression of reflexive pain responses, thermal hyperalgesia and mechanical allodynia, throughout the chronic phase of SCI (up to 12 weeks post-injury) showed that chronic neuropathic pain persists following mild SCI despite the presence of only minor disruptions to locomotor abilities. The lack of changes in objective measurements and observations of the animals' visible state allow us to infer that the functional data obtained were not influenced by any discomfort experienced by the animals. These findings were consistent with previous observations in chronic SCI mice (Castany et al., 2023), confirming their proper development and ensuring that subsequently collected serum samples corresponded to mice expressing chronic neuropathic pain during the chronic phase of SCI. It is important to mention that while humans may take up to 6 months to transition to the chronic phase of SCI (Ahuja et al., 2017), the temporal progression of SCI phases in murine experimental models is briefer. The immediate and acute phases typically last for approximately 2–3 weeks post-injury (Taoka and Okajima, 1998), followed by an intermediate phase spanning from 3 to 6 weeks (Young, 2002). Following this, the chronic phase generally begins at around 6–8 weeks

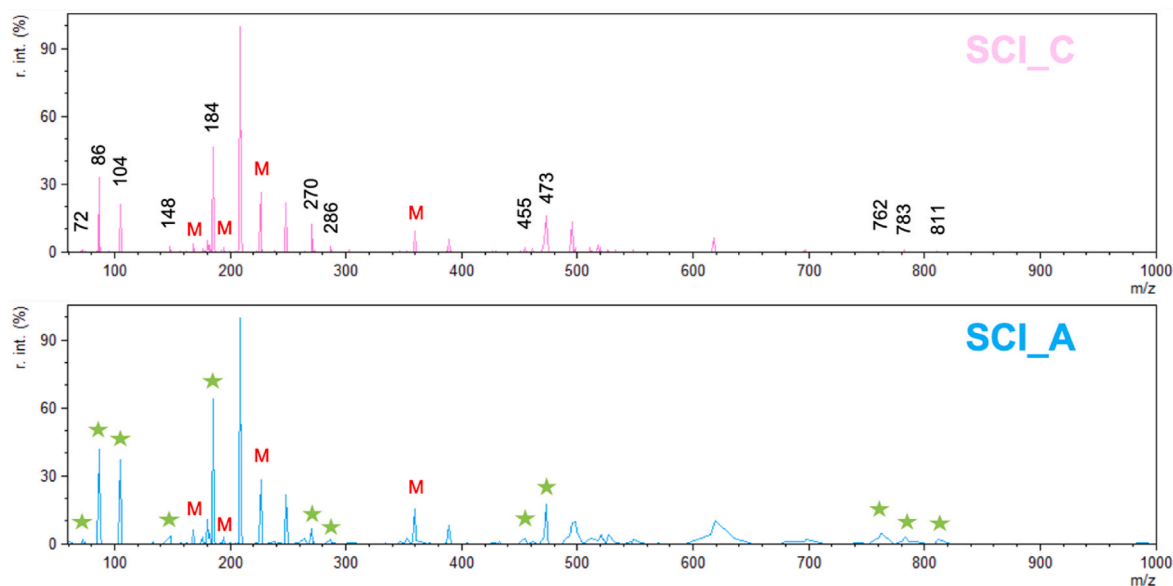


Fig. 8. Representative serum mass spectra of SCI mice in both chronic and acute phases of the injury obtained by MALDI-TOF MS. Differences between the SCI_C and SCI_A groups can be observed. The stars indicate the group with the highest intensity of some of the peaks. M refers to the peaks of the matrix.

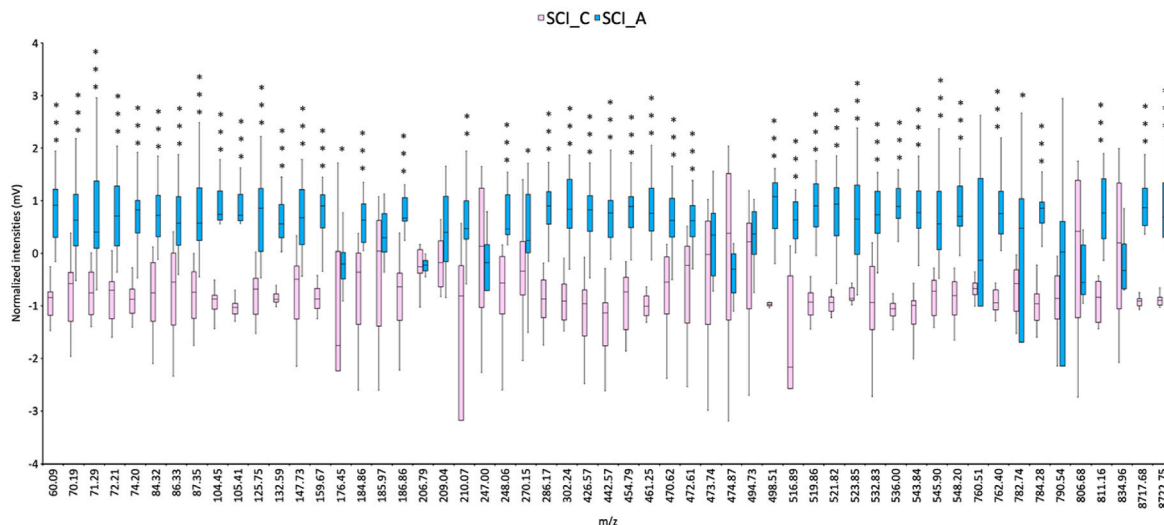


Fig. 9. Intensities of the most relevant peaks found in the serum mass spectra obtained by MALDI-TOF MS. Data shown as the median of each group \pm IQR. (* $p < 0.05$, ** $p < 0.01$, *** $p < 0.001$). Experimental groups: SCI_C (n = 14) and SCI_A (n = 15) serum samples of each animal were analyzed by triplicate.

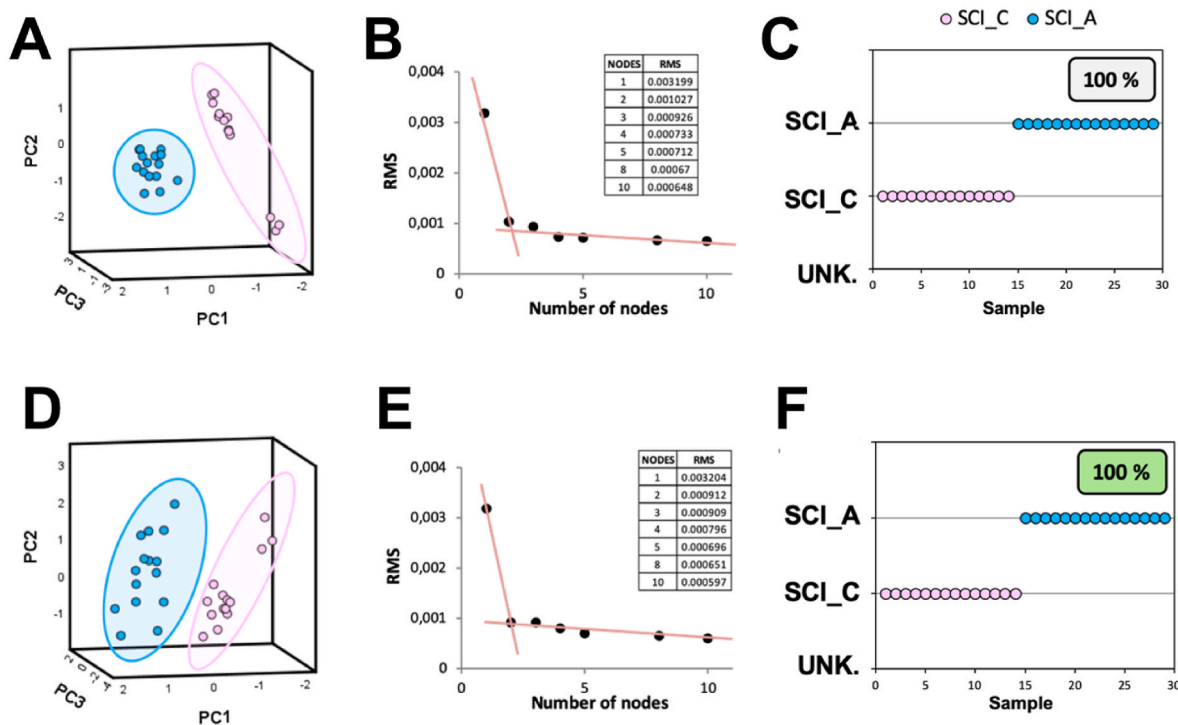


Fig. 10. Serum spectral profile analyses coupling MALDI-TOF MS data and ANN analysis using databases of SCI_C and SCI_A samples. (A) PCA using 55 m/z values of mass spectrum data obtained from chronic and acute spinal cord injury models; (B) plot of the RMS against the number of nodes in the hidden layer corresponding to the analysis using 55 inputs. Three nodes in the hidden layer were used in the analyses; (C) detail of the ANN classification output based on the 55 peaks. (D) PCA using 42 m/z values of mass spectrum data obtained from chronic and acute spinal cord injury models; (E) plot of the RMS against the number of nodes in the hidden layer corresponding to the analysis using 42 inputs. Three nodes in the hidden layer were used in the analyses; (F) detail of the ANN classification output based on the 42 peaks. Experimental groups: SCI_C (n = 14) and SCI_A (n = 15).

Table 2
Serum peaks relevant to distinguish between chronic and acute pain in spinal cord injuries.

RELEVANT M/Z FOR THE CLASSIFICATION (Da)
60.09, 70.19, 71.29, 72.21, 74.20, 84.32, 86.33, 87.35, 104.45, 105.41, 125.75, 147.73, 159.67, 176.45, 184.86, 186.86, 206.79, 209.04, 286.17, 302.24, 426.57, 442.57, 454.79, 461.25, 470.62, 474.87, 498.51, 516.89, 519.86, 521.82, 532.83, 536.00, 543.84, 548.84, 548.20, 760.51, 762.40, 782.74, 784.28, 811.16, 8717.68, 8722.75

of the injury (Arnold and Hagg, 2011). Therefore, given that the serum samples were collected 12 weeks after injury, we can be confident that they were suitable for assessing the proposed methodology (MALDI-TOF MS fingerprints coupled with ANN).

With regards to the first serum spectral profile analysis, visual examination of mass spectra of both SCI_C mice and Sham_C control mice showed similar profiles and there was no indication that any individual peaks might serve as a group marker. This observation has been previously documented in acute pathological pain mouse models (Deulofeu et al., 2023). Specifically, no single peaks appear to align with group markers in models of pathological pain, including peripheral neuropathic pain (CCI - chronic constriction injury of the sciatic nerve), central neuropathic pain (acute SCI - spinal cord injury), and nociplastic pain states (RIM - reserpine-induced myalgia mice, and ASI - mice injected with intramuscular acid saline solution) (Deulofeu et al., 2023). As has been discussed by other authors in prior experiments, the challenge of clearly delineating a structural m/z signal for SCI_C is yet another example of the current elusiveness of optimal pain biomarkers (Scherl, 2015). Given this failure, the proposed approach of concurrently measuring multiple compounds to discern overarching patterns (Deulofeu et al., 2023; Sisignano et al., 2019) rather than focusing solely on individual biomolecules emerges as the most suitable course of action once again. Expanding on the observational results, a detailed analysis of the mass spectra was performed, producing a database of 322 m/z values with signal-to-noise ratios (S/N) ≥ 3 . After removing irrelevant data, 113 m/z values were retained. Box-plot analyses showed significant differences in the intensities of 12 m/z values between the groups. PCA was applied to uncover distinct metabolomic patterns, revealing two clear clusters, despite some overlap. Applying this multivariate analysis approach, most of the SCI_C samples could be clearly differentiated from their respective Sham_C. These results suggest the potential presence of metabolomic patterns within these mass spectra that may be analyzed by ANN to develop a classification method. This multivariate analysis approach proved to be highly effective in distinguishing between samples of SCI-induced chronic pathological pain mice and their corresponding sham controls.

The subsequent step involved combining MALDI-TOF mass spectral profiles with ANN analysis in order to develop a methodology that could distinguish between SCI_C samples and those of Sham_C. Given this success, we proceeded to evaluate whether reducing the number of variables could still yield the same result. The analysis was then conducted using the 53 remaining signals. Although a classification rate above 90% was obtained, the success rate was lower compared to using the full database. This suggests that the 113 m/z peaks extracted from the mass spectra provide valuable information for sample differentiation through ANN analysis, potentially representing the serum spectral profile or fingerprint of the chronic phase of SCI. Collectively these findings suggest that significant insights gleaned from mass spectra can serve as inputs for ANN analyses, facilitating the differentiation between serum samples obtained from SCI_C and those from Sham_C healthy mice.

Although all samples were accurately classified using information from the mass spectra alone, the influence of pain response data on the discrimination of the samples by ANN analysis was evaluated. In other words, considering the evidence that functional data can either enhance or diminish the success of ANN classification of pathological pain samples (Deulofeu et al., 2023), outputs from functional analyses of chronic models were integrated with fingerprint data to assess their influence on the classification of the SCI-induced chronic neuropathic pain model. As a result, the success rate of the ANN classification of the SCI-induced chronic neuropathic pain model did not improve after integrating functional and fingerprint data suggesting that reflexive pain response data (thermal hyperalgesia and mechanical allodynia) did not offer significant information for the classification of samples by ANN. These findings diverge from those observed in acute models of pathological pain, where the inclusion of functional data alongside those of CCI, RIM6, ASI, or acute SCI enhanced the classification capacity,

particularly in terms of thermal hyperalgesia (Deulofeu et al., 2023). However, it is important to note that in the present study, the decrease in success rates may be attributed to the slight recovery observed in the animals during the two functional tests at the end of the experimental period. In fact, these findings should be interpreted positively as they provide robust evidence for the presence of SCI-related chronic pathological pain without the need for functional data. In other words, the gradual and consistent decrease in reflexive pain responses leading up to the chronic phase may misguidedly lead to the conclusion that there is an absence of neuropathic pain. However, the information provided by the specific spectral profile of chronic SCI indicates the presence of a pathological process that, if replicated in humans, should prompt clinicians to continue with necessary interventions despite the absence of reflexive responses. This reduction in reflexive pain responses has previously been documented (Castany et al., 2023), although the chronic phase typically sees a rise in non-reflexive pain responses, such as depression, anxiety, and cognitive impairment (Castany et al., 2023; Wu et al., 2014a, 2014b, 2016). Given these findings, we believe that future experiments should focus on enhancing this methodology by integrating non-reflexive pain responses instead of reflexive ones in models of chronic pathological pain. It is hoped that this will eventually make it possible to distinguish between spectral profiles associated with non-reflexive pain responses from those linked to mood disorders that do not correlate with pain.

After establishing a reliable methodology that combines MALDI-TOF MS with ANN analysis to differentiate between samples of SCI-induced chronic neuropathic and sham chronic conditions, our focus turned to determining its potential in discerning the distinct pain profiles across different phases of SCI. To this end, we investigated whether this methodology could effectively discriminate between the characteristics associated with both chronic and acute phases of SCI. Serum samples from the SCI_C that had been obtained so far were analyzed together with stored serum samples obtained from SCI mice put down three weeks after injury (SCI_A) in previous experiments (Deulofeu et al., 2023). For the present study, we only used serum aliquots from these acute SCI mice to achieve the new objective of distinguishing between samples of SCI_C and SCI_A, thereby avoiding the need to use additional animals. As a result, the analysis of serum samples via MALDI-TOF MS, followed by statistical analysis using ANN, has also made it possible to distinguish between chronic and acute SCI-induced neuropathic pain within the same type of lesion without the need to rely on structural biomarkers or to incorporate additional functional data. Understanding the phase of the pathophysiological process in a patient is clinically relevant as this is important additional information for physicians when deciding on the most appropriate treatment. Furthermore, and although not the primary focus of the current study, the spectral profiles could prove useful in identifying structural biomarkers that may serve as pharmacological targets. Leveraging ANN and other machine learning models could help define specific molecular biomarker ranges that play a crucial role in disease detection. In other words, certain characteristic m/z values in molecular profiles may correspond to key biomolecules associated with the disease. These molecules could then be sequenced using tandem MS and advanced sequencing techniques. Future research should aim not only at identifying specific molecular profiles but also at pinpointing pain-specific biomarkers within the spectral data, employing techniques such as MALDI-TOF MS/MS. Although electrospray ionization (ESI) is commonly used as ion source in tandem mass spectrometry-based proteomic studies in biomedical research (Nadler et al., 2017), MALDI-TOF/TOF remains a relatively fast and straightforward alternative for qualitative and quantitative analysis of biomolecules (Gogichaeva and Alterman, 2012, 2019; Darie-Ion et al., 2022), to study protein-protein interactions (PPIs), and post-translational modifications (PTMs). Peptides and proteins hold potential as clinical biomarkers due to advantageous features, such as user-friendly sample preparation (Dave et al., 2011; Darie-Ion et al., 2022), preservation of non-covalent interactions, and high sensitivity,

along with high-throughput screening capabilities for rapid data acquisition (Giampa and Sgobba, 2020; Darie-Ion et al., 2022). These techniques have been successfully applied to analyze biofluids such as serum, plasma, and urine, proving effective across a wide range of diseases (Darie-Ion et al., 2022).

The decision to use female mice is, in part, an acknowledgement of the greater susceptibility of females to emotional comorbidities in pain disorders (Goesling et al., 2013; Miller and Cano, 2009). Evidence shows that females experience greater pain prevalence and severity, and female mice exhibit heightened hypersensitivity after SCI compared to males (Lee et al., 2023). Ovarian hormones and neuroimmune mechanisms, such as prolactin receptor signalling, may contribute to these sex differences in pain (Guindon et al., 2019; Sanoja and Cervero, 2008; Paige et al., 2020). Transcriptomic analyses also reveal distinct gene expression related to neuropathic pain between sexes (Dai et al., 2022), suggesting that oestrogen prolongs pain sensitivity in females, while testosterone reduces it in males (Paige et al., 2020). Despite these facts, chronic pain research in women has been historically underrepresented (Osborne and Davis, 2022; Li et al., 2023). The more frequent pain and lower thresholds experienced by women (Casale et al., 2021) also increases the case for sex-specific approaches in pain research and treatment (Hoffmann et al., 2022). With regard to the potential effects of ovarian cycle phases on experimental female outcomes, although female subjects are underrepresented in preclinical studies, recent findings challenge the notion that the oestrous cycle significantly affects experimental outcomes. Behavioural assays showed no major differences across oestrous phases in anxiety, depression-like behaviours, or social interaction (Zeng et al., 2023; Zhao et al., 2021), and female mice did not exhibit greater variability than males in most traits (Prendergast et al., 2014). While mild effects of the oestrous cycle on pain response may exist (Martin, 2009), studies indicate that female mice can be reliably used in neuropathic pain research without strict oestrous cycle monitoring (Prendergast et al., 2014; Sanoja and Cervero, 2008). Consistency in this aspect is key for the application of the methodology we have developed, proving its potential applicability regardless of the ovarian cycle.

5. Conclusions

These findings emphasize the potential of MALDI-TOF MS integrated with ANNs as a diagnostic approach for chronic neuropathic pain, potentially facilitating the discovery of biomarkers and the development of new treatments.

The current research undertaken in a mice model gives rise to interesting questions that will need to be studied to better understand pain in humans. Testing will be required to determine whether the methodology presented here may be of use to physicians in clearly identifying the phase of the pathophysiological process that the patients are experiencing, so assisting them in the selection of the most appropriate interventions. Furthermore, the spectral profiles obtained through this methodology may prove useful in identifying structural biomarkers that could become pharmacological targets. With the high success rate observed, future experiments could concentrate solely on the spectral profiles obtained in this study, potentially playing a pivotal role in the identification of specific molecular biomarkers through association with significant peaks for subsequent structural sequencing (Cho et al., 2015; Dettmer et al., 2007), which may lead to the development of new more specific drugs in a landscape where there are currently insufficient suitable treatments available (Spinal Cord Injury (SCI) 2016 facts and figures at a glance, 2016; Suzuki and Sakai, 2021). The World Health Organization (WHO) estimates that over 15 million people are currently living with SCI, with most cases resulting from trauma, mimicking the contusion model studied here, thus illustrating the clinical relevance of the present study. The WHO emphasizes the importance of preventing, diagnosing at an early stage, and treating SCI-related secondary conditions to improve quality of life, as a response

to the chronic state that many patients are forced to live with in the absence of treatment for the primary conditions. Given that the main aim of this study was to develop a potential clinical decision support tool for enhancing diagnostics and potentially identifying new therapeutic targets, it aligns with the WHO's priorities. Recent statistical projections up to 2030 using Bayesian age-period-cohort analysis have further emphasized the urgency, revealing an upward trend in age-standardized incidence rates of SCI until 2030 (Liu et al., 2023).

CRedit authorship contribution statement

Meritxell Deulofeu: Writing – review & editing, Validation, Software, Investigation, Formal analysis, Data curation. **Eladia M. Peña-Méndez:** Writing – review & editing, Validation, Software, Methodology, Formal analysis. **Petr Vaňhara:** Writing – review & editing, Validation, Resources, Funding acquisition, Formal analysis. **Josef Havel:** Writing – review & editing, Validation, Resources, Funding acquisition. **Lukáš Morán:** Writing – review & editing, Visualization, Validation, Investigation, Data curation. **Lukáš Pečinka:** Writing – review & editing, Visualization, Validation, Investigation, Data curation. **Anna Bagó-Mas:** Writing – review & editing, Visualization, Validation, Investigation, Formal analysis, Data curation. **Enrique Verdú:** Writing – review & editing, Resources, Methodology. **Victoria Salvadó:** Writing – review & editing, Supervision, Resources, Project administration, Methodology, Formal analysis, Conceptualization. **Pere Boadas-Vaello:** Writing – review & editing, Writing – original draft, Validation, Supervision, Software, Resources, Project administration, Methodology, Funding acquisition, Formal analysis, Data curation, Conceptualization.

Ethics statement

The animal study protocol was approved by the Animal Experimentation Ethics Committee of the University of Barcelona and the *Generalitat de Catalunya* (Government of Catalonia) (DAAM number 8884).

Funding sources

This work was supported by the by the University of Girona [MPCUdG2016/087] and La MARATÓ de TV3 Foundation [201705.30.31] in Catalonia, as well as from Masaryk University [MUNI/A/1598/2023, MUNI/A/1398/2021, MUNI/A/1412/2021] in Brno, Czech Republic.

Declaration of competing interest

The authors declare no conflicts of interest.

Acknowledgments

The authors express gratitude to the personnel at the animal care facility of the University of Barcelona (Campus Bellvitge, Catalonia, Spain) for their adept technical support. Additionally, the Mass Spectrometry Core Facility of FNUSA-ICRC (Brno, Czech Republic) is acknowledged for their valuable support and assistance in this Endeavor.

Data availability

Data will be made available on request.

References

- Agatonovic-Kustrin, S., Beresford, R., 2000. Basic concepts of artificial neural network (ANN) modelling and its application in pharmaceutical research. *J. Pharm. Biomed. Anal.* 22, 717–727. [https://doi.org/10.1016/S0731-7085\(99\)00272-1](https://doi.org/10.1016/S0731-7085(99)00272-1).

- Ahuja, C.S., Wilson, J.R., Nori, S., Kotter, M.R.N., Druschel, C., Curt, A., Fehlings, M.G., 2017. Traumatic spinal cord injury. *Nat Rev Dis Primers* 3, 17018. <https://doi.org/10.1038/nrdp.2017.18>.
- Amato, F., López, A., Peña-Méndez, E.M., Vanhara, P., Hampl, A., Havel, J., 2013. Artificial neural networks in medical diagnosis. *J. Appl. Biomed.* 11, 47–58. <https://doi.org/10.2478/v10136-012-0031-x>.
- Arnold, S.A., Hagg, T., 2011. Anti-inflammatory treatments during the chronic phase of spinal cord injury improve locomotor function in adult mice. *J. Neurotrauma* 28 (9), 1995–2002. <https://doi.org/10.1089/neu.2011.1888>.
- Attal, N., 2019. Pharmacological treatments of neuropathic pain: the latest recommendations. *Rev. Neurol. (Paris)* 175, 46–50. <https://doi.org/10.1016/j.neurol.2018.08.005>.
- Bäckryd, E., Ghafouri, B., Carlsson, A.K., Olausson, P., Gerdle, B., 2015. Multivariate proteomic analysis of the cerebrospinal fluid of patients with peripheral neuropathic pain and healthy controls - a hypothesis-generating pilot study. *J. Pain Res.* 8, 321–333. <https://doi.org/10.2147/JPR.S82970>.
- Bagó-Mas, A., Korimová, A., Deulofeu, M., Verdú, E., Fiol, N., Svobodová, V., Dubový, P., Boadas-Vaello, P., 2022. Polyphenolic grape stalk and coffee extracts attenuate spinal cord injury-induced neuropathic pain development in ICR-CD1 female mice. *Sci. Rep.* 12 (1), 14980. <https://doi.org/10.1038/s41598-022-19109-4>.
- Basheer, I.A., Hajmeer, M., 2000. Artificial neural networks: fundamentals, computing, design, and application. *J. Microbiol. Methods* 43 (1), 3–31. [https://doi.org/10.1016/S0167-7012\(00\)00201-3](https://doi.org/10.1016/S0167-7012(00)00201-3).
- Basso, D.M., Fisher, L.C., Anderson, A.J., Jakeman, L.B., McTigue, D.M., Popovich, P.G., 2006. Basso Mouse Scale for locomotion detects differences in recovery after spinal cord injury in five common mouse strains. *J. Neurotrauma* 23 (5), 635–659. <https://doi.org/10.1089/neu.2006.23.635>.
- Burke, D., Fullen, B.M., Stokes, D., Lennon, O., 2017. Neuropathic pain prevalence following spinal cord injury: a systematic review and meta-analysis. *Eur. J. Pain* 21 (1), 29–44. <https://doi.org/10.1002/ejp.905>.
- Cardenas, D.D., Felix, E.R., 2009. Pain after spinal cord injury: a review of classification, treatment approaches, and treatment assessment. *Pharm. Manag. PM R* 1 (12), 1077–1090. <https://doi.org/10.1016/j.pmrj.2009.07.002>.
- Casale, R., Atzeni, F., Bazzichi, L., Beretta, G., Costantini, E., Sacerdote, P., Tassorelli, C., 2021. Pain in women: a perspective review on a relevant clinical issue that deserves prioritization. *Pain Ther* 10 (1), 287–314. <https://doi.org/10.1007/s40122-021-00244-1>.
- Castany, S., Bagó-Mas, A., Vela, J.M., Verdú, E., Bretová, K., Svobodová, V., Dubový, P., Boadas-Vaello, P., 2023. Transient reflexive pain responses and chronic affective nonreflexive pain responses associated with neuroinflammation processes in both spinal and supraspinal structures in spinal cord-injured female mice. *Int. J. Mol. Sci.* 24 (2), 1761. <https://doi.org/10.3390/ijms24021761>.
- Chae, Y., Park, H.J., Lee, I.S., 2022. Pain modalities in the body and brain: current knowledge and future perspectives. *Neurosci. Biobehav. Rev.* 139, 104744. <https://doi.org/10.1016/j.neubiorev.2022.104744>.
- Cho, Y.T., Su, H., Wu, W.J., Wu, D.C., Hou, M.F., Kuo, C.H., Shiea, J., 2015. Biomarker characterization by MALDI-TOF/MS. *Adv. Clin. Chem.* 69, 209–254. <https://doi.org/10.1016/bs.acc.2015.01.001>.
- Cohen, S.P., Mao, J., 2014. Neuropathic pain: mechanisms and their clinical implications. *BMJ* 348, f7656. <https://doi.org/10.1136/bmj.f7656>.
- Dai, W., Huang, S., Luo, Y., Cheng, X., Xia, P., Yang, M., Zhao, P., Zhang, Y., Lin, W.J., Ye, X., 2022. Sex-specific transcriptomic signatures in brain regions critical for neuropathic pain-induced depression. *Front. Mol. Neurosci.* 15, 886916. <https://doi.org/10.3389/fnmol.2022.886916>.
- Daric-Ion, L., Whitham, D., Jayathirtha, M., Rai, Y., Neagu, A.N., Daric, C.C., Petre, B.A., 2022. Applications of MALDI-MS/MS-based proteomics in biomedical research. *Molecules* 27 (19), 6196. <https://doi.org/10.3390/molecules27196196>.
- Dave, K.A., Headlam, M.J., Wallis, T.P., Gorman, J.J., 2011. Preparation and analysis of proteins and peptides using MALDI TOF/TOF mass spectrometry. *Curr Protoc Protein Sci.* <https://doi.org/10.1002/0471140864.ps1613s63>. Chapter 16:16.13.1–16.13.21.
- Detmer, K., Aronov, P.A., Hammock, B.D., 2007. Mass spectrometry-based metabolomics. *Mass Spectrom. Rev.* 26 (1), 51–78. <https://doi.org/10.1002/mas.20108>.
- Deulofeu, M., García-Cuesta, E., Peña-Méndez, E.M., Conde, J.E., Jiménez-Romero, O., Verdú, E., Serrando, M.T., Salvadó, V., Boadas-Vaello, P., 2021. Detection of SARS-CoV-2 infection in human nasopharyngeal samples by combining MALDI-TOF MS and artificial intelligence. *Front. Med.* 8, 661358. <https://doi.org/10.3389/fmed.2021.661358>.
- Deulofeu, M., Kolářová, L., Salvadó, V., María Peña-Méndez, E., Almási, M., Štokr, M., Pour, L., Boadas-Vaello, P., Ševčíková, S., Havel, J., Vanhara, P., 2019. Rapid discrimination of multiple myeloma patients by artificial neural networks coupled with mass spectrometry of peripheral blood plasma. *Sci. Rep.* 9, 7975. <https://doi.org/10.1038/s41598-019-44215-1>.
- Deulofeu, M., Peña-Méndez, E.M., Vanhara, P., Havel, J., Morán, L., Pečinka, L., Bagó-Mas, A., Verdú, E., Salvadó, V., Boadas-Vaello, P., 2023. Artificial Neuronal Networks coupled with MALDI-TOF MS serum fingerprinting to classify and diagnose pathological pain subtypes in preclinical models. *ACS Chem. Neurosci.* 14 (2), 300–311. <https://doi.org/10.1021/acscchemneuro.2c00665>.
- Dixon, W.J., 1980. Efficient analysis of experimental observations. *Annu. Rev. Pharmacol. Toxicol.* 20, 441–462. <https://doi.org/10.1146/annurev.pa.20.040180.002301>.
- Duncan, M.W., Nedelkov, D., Walsh, R., Hattan, S.J., 2016. Applications of MALDI mass spectrometry in clinical chemistry. *Clin. Chem.* 62, 134–143. <https://doi.org/10.1373/clinchem.2015.239491>.
- Failde, I., Dueñas, M., Ribera, M.V., Gálvez, R., Mico, J.A., Salazar, A., de Sola, H., Pérez, C., 2018. Prevalence of central and peripheral neuropathic pain in patients attending pain clinics in Spain: factors related to intensity of pain and quality of life. *J. Pain Res.* 11, 1835–1847. <https://doi.org/10.2147/JPR.S159729>.
- Giampà, M., Sgobba, E., 2020. Insight to functional conformation and noncovalent interactions of protein-protein assembly using MALDI mass spectrometry. *Molecules* 25, 4979.
- Goesling, J., Clauw, D.J., Hassett, A.L., 2013. Pain and depression: an integrative review of neurobiological and psychological factors. *Curr Psychiatry Rep* 15, 421. <https://doi.org/10.1007/s11920-013-0421-0>.
- Gogichava, N.V., Alterman, M.A., 2012. Amino acid analysis by means of MALDI TOF mass spectrometry or MALDI TOF/TOF tandem mass spectrometry. *Methods Mol. Biol.* 828, 121–135. https://doi.org/10.1007/978-1-61779-445-2_12.
- Gogichava, N.V., Alterman, M.A., 2019. Amino acid analysis by means of MALDI TOF mass spectrometry or MALDI TOF/TOF tandem mass spectrometry. *Methods Mol. Biol.* 2030, 17–31. https://doi.org/10.1007/978-1-4939-9639-1_3.
- Guindon, J., Blanton, H., Brauman, S., Donckels, K., Narasimhan, M., Benamar, K., 2019. Sex differences in a rodent model of HIV-1-Associated neuropathic pain. *Int. J. Mol. Sci.* 20 (5), 1196. <https://doi.org/10.3390/ijms20051196>.
- Hoffmann, D.E., Fillingim, R.B., Veasley, C., 2022. The woman who cried pain: do sex-based disparities still exist in the experience and treatment of pain? *J. Law Med. Ethics* 50 (3), 519–541. <https://doi.org/10.1017/jme.2022.91>.
- Houska, J., Peña-Méndez, E.M., Hernandez-Fernaud, J.R., Salido, E., Hampl, A., Havel, J., Vanhara, P., 2014. Tissue profiling by nanogold-mediated mass spectrometry and artificial neural networks in the mouse model of human primary hyperalgesia 1. *J. Appl. Biomed.* 12, 119–125. <https://doi.org/10.1016/j.jab.2013.12.001>.
- Hunt, C., Moman, R., Peterson, A., Wilson, R., Covington, S., Mustafa, R., Murad, M.H., Hooten, W.M., 2021. Prevalence of chronic pain after spinal cord injury: a systematic review and meta-analysis. *Reg. Anesth. Pain Med.* 46 (4), 328–336. <https://doi.org/10.1136/rapm-2020-101960>.
- Lee, S.E., Greenough, E.K., Oancea, P., Scheinfeld, A.R., Douglas, A.M., Gaudet, A.D., 2023. Sex differences in pain: spinal cord injury in female and male mice elicits behaviors related to neuropathic pain. *J. Neurotrauma* 40 (9–10), 833–844. <https://doi.org/10.1089/neu.2022.0482>.
- Li, J.X.L., Wang, X., Henry, A., Anderson, C.S., Hammond, N., Harris, K., Liu, H., Loffler, K., Myburgh, J., Pandian, J., Smyth, B., Venkatesh, B., Carcel, C., Woodward, M., 2023. Sex differences in pain expressed by patients across diverse disease states: individual patient data meta-analysis of 33,957 participants in 10 randomized controlled trials. *Pain* 164 (8), 1666–1676. <https://doi.org/10.1097/j.pain.0000000000002884>.
- Liu, X., Locasale, J.W., 2017. Metabolomics: a primer. *Trends Biochem. Sci.* 42 (4), 274–284. <https://doi.org/10.1016/j.tibs.2017.01.004>.
- Liu, Y., Yang, X., He, Z., Li, J., Li, Y., Wu, Y., Manyande, A., Feng, M., Xiang, H., Liu, Y., Yang, X., He, Z., Li, J., Li, Y., Wu, Y., Manyande, A., Feng, M., Xiang, H., 2023. Spinal cord injury: global burden from 1990 to 2019 and projections up to 2030 using Bayesian age-period-cohort analysis. *Front. Neurol.* 14, 1304153. <https://doi.org/10.3389/fneur.2023.1304153>.
- Martin, V.T., 2009. Ovarian hormones and pain response: a review of clinical and basic science studies. *Gen. Med.* 6 (Suppl. 2), 168–192. <https://doi.org/10.1016/j.genm.2009.03.006>.
- Miller, L.R., Cano, A., 2009. Comorbid chronic pain and depression: who is at risk? *J. Pain* 10, 619–627. <https://doi.org/10.1016/j.jpain.2008.12.007>.
- Monakhova, Y.B., Goryacheva, I.Y., 2016. Chemometric analysis of luminescent quantum dots systems: long way to go but first steps taken. *TrAC, Trends Anal. Chem.* 82, 164–174. <https://doi.org/10.1016/j.trac.2016.05.017>.
- Morlion, B., Coluzzi, F., Aldington, D., Kocot-Kepska, M., Pergolizzi, J., Mangas, A.C., Ahlbeck, K., Kalso, E., 2018. Pain chronification: what should a non-pain medicine specialist know? *Curr. Med. Res. Opin.* 34, 1169–1178. <https://doi.org/10.1080/03007995.2018>.
- Morton, D.B., Griffiths, P.H., 1985. Guidelines on the recognition of pain, distress and discomfort in experimental animals and an hypothesis for assessment. *Vet. Rec.* 116, 431–436. <https://doi.org/10.1038/s41598-022-13968-7>.
- Murray, R.F., Asghari, A., Egorov, D.D., Rutkowski, S.B., Siddall, P.J., Soden, R.J., Ruff, R., 2007. Impact of spinal cord injury on self-perceived pre- and postmorbid cognitive, emotional and physical functioning. *Spinal Cord* 45, 429–436. <https://doi.org/10.1038/sj.sc.3102022>.
- Nadler, W.M., Waidelich, D., Kerner, A., Hanke, S., Berg, R., Trumpp, A., Rösl, C., 2017. MALDI versus ESI: the impact of the ion source on peptide identification. *J. Proteome Res.* 16 (3), 1207–1215. <https://doi.org/10.1021/acs.jproteome.6b00805>.
- Norenberg, M.D., Smith, J., Marcillo, A., 2004. The pathology of human spinal cord injury: defining the problems. *J. Neurotrauma* 21, 429–440.
- Norris, J.L., Cornett, D.S., Mobley, J.A., Andersson, M., Seeley, E.H., Chaurand, P., Caprioli, R.M., 2007. Processing MALDI mass spectra to improve mass spectral direct tissue analysis. *Int. J. Mass Spectrom.* 260, 212–221. <https://doi.org/10.1016/j.ijms.2006.10.005>.
- Osborne, N.R., Davis, K.D., 2022. Sex and gender differences in pain. *Int. Rev. Neurobiol.* 164, 277–307. <https://doi.org/10.1016/bs.irn.2022.06.013>.
- Paige, C., Barba-Escobedo, P.A., Mecklenburg, J., Patil, M., Goffin, V., Grattan, D.R., Dussor, G., Akopian, A.N., Price, T.J., 2020. Neuroendocrine mechanisms governing sex differences in hyperalgesic priming involve prolactin receptor sensory neuron signaling. *J. Neurosci.* 40 (37), 7080–7090. <https://doi.org/10.1523/JNEUROSCI.1499-20.2020>.

- Pirvulescu, I., Biskis, A., Candido, K.D., Knezevic, N.N., 2022. Overcoming clinical challenges of refractory neuropathic pain. *Expert Rev. Neurother.* 22, 595–622. <https://doi.org/10.1080/14737175.2022.2105206>.
- Prendergast, B.J., Onishi, K.G., Zucker, I., 2014. Emale mice liberated for inclusion in neuroscience and biomedical research. *Neurosci. Biobehav. Rev.* 40, 1–5. <https://doi.org/10.1016/j.neubiorev.2014.01.001>.
- Rivers, C.S., Fallah, N., Noonan, V.K., Whitehurst, D.G., Schwartz, C.E., Finkelstein, J.A., Craven, B.C., Ethans, K., O'Connell, C., Truchon, B.C., Ho, C., Linassi, A.G., Short, C., Tsai, E., Drew, B., Ahn, H., Dvorak, M.F., Paquet, J., Fehlings, M.G., Noreau, L., Rhscir, Network, 2018. Health conditions: effect on function, health-related quality of life, and life satisfaction after traumatic spinal cord injury. A prospective observational registry cohort study. *Arch. Phys. Med. Rehabil.* 99, 443–451. <https://doi.org/10.1016/j.apmr.2017.06.012>.
- Sanoja, R., Cervero, F., 2008. Estrogen modulation of ovariectomy-induced hyperalgesia in adult mice. *Eur. J. Pain* 12 (5), 573–581. <https://doi.org/10.1016/j.ejpain.2007.09.003>.
- Saurí, J., Chamorro, A., Gilabert, A., Gifre, M., Rodriguez, N., Lopez-Blazquez, R., Curcoll, L., Benito-Penalva, J., Soler, D., 2017. Depression in individuals with traumatic and nontraumatic spinal cord injury living in the community. *Arch. Phys. Med. Rehabil.* 98, 1165–1173. <https://doi.org/10.1016/j.apmr.2016.11.011>.
- Scherl, A., 2015. Clinical protein mass spectrometry. *Methods* 81, 3–14. <https://doi.org/10.1016/j.ymeth.2015.02.015>.
- Schrimep-Rutledge, A.C., Codreanu, S.G., Sherrod, S.D., McLean, J.A., 2016. Untargeted metabolomics strategies-challenges and emerging directions. *J. Am. Soc. Mass Spectrom.* 27 (12), 1897–1905. <https://doi.org/10.1007/s13361-016-1469-y>.
- Sisignano, M., Lötsch, J., Parnham, M.J., Geisslinger, G., 2019. Potential biomarkers for persistent and neuropathic pain therapy. *Pharmacol. Ther.* 199, 16–29. <https://doi.org/10.2147/JPR.S82970>.
- Smith, S.M., Dworkin, R.H., Turk, D.C., Baron, R., Polydefkis, M., Tracey, I., Borssook, D., Edwards, R.R., Harris, R.E., Wager, T.D., 2017. The potential role of sensory testing, skin biopsy, and functional brain imaging as biomarkers in chronic pain clinical trials: IMMEDIATE considerations. *J. Pain* 18, 757–777. <https://doi.org/10.1016/j.jpain.2017.02.429>.
- Soler-Martínez, R., Deulofeu, M., Bagó-Mas, A., Dubový, P., Verdú, E., Fiol, N., Boadas-Vaello, P., 2022. Central neuropathic pain development modulation using coffee extract major polyphenolic compounds in spinal-cord-injured female mice. *Biology* 11 (11), 1617. <https://doi.org/10.3390/biology11111617>.
- Spinal Cord Injury (SCI) 2016 facts and figures at a glance. *J. Spinal Cord Med.* 39 (4), 2016, 493–494. <https://doi.org/10.1080/10790268.2016.1210925>.
- Suzuki, H., Sakai, T., 2021. Current concepts of stem cell therapy for chronic spinal cord injury. *Int. J. Mol. Sci.* 22 (14), 7435. <https://doi.org/10.3390/ijms22147435>.
- Taoka, Y., Okajima, K., 1998. Spinal cord injury in the rat. *Prog. Neurobiol.* 56 (3), 341–358. [https://doi.org/10.1016/s0301-0082\(98\)00049-5](https://doi.org/10.1016/s0301-0082(98)00049-5).
- Treede, R.D., Rief, W., Barke, A., Aziz, Q., Bennett, M.I., Benoliel, R., Cohen, M., Evers, S., Finnerup, N.B., First, M.B., 2019. Chronic pain as a symptom or a disease: the IASP classification of chronic pain for the international classification of diseases (ICD-11). *Pain* 160, 19–27. <https://doi.org/10.1097/j.pain.0000000000001384>.
- Vall, J., Batista-Braga, V.A., Almeida, P.C., 2006. Central neuropathic pain and its relation to the quality of life of a person with a traumatic spinal cord injury. *Rev. Neurol.* 42, 525–529.
- World Health Organization – WHO. Spinal cord injury. <https://www.who.int/news-room/fact-sheets/detail/spinal-cord-injury>. (Accessed 23 April 2024).
- Wu, J., Stoica, B.A., Luo, T., Sabirzhanov, B., Zhao, Z., Guanciale, K., Nayar, S.K., Foss, C. A., Pomper, M.G., Faden, A.I., 2014a. Isolated spinal cord contusion in rats induces chronic brain neuroinflammation, neurodegeneration, and cognitive impairment. Involvement of cell cycle activation. *Cell Cycle* 13, 2446–2458. <https://doi.org/10.4161/cc.29420>.
- Wu, J., Zhao, Z., Kumar, A., Lipinski, M.M., Loane, D.J., Stoica, B.A., Faden, A.I., 2016. Endoplasmic Reticulum Stress and Disrupted Neurogenesis in the brain are associated with cognitive impairment and depressive-like behavior after spinal cord injury. *J. Neurotrauma* 33, 1919–1935. <https://doi.org/10.1089/neu.2015.4348>.
- Wu, J., Zhao, Z., Sabirzhanov, B., Stoica, B.A., Kumar, A., Luo, T., Skovira, J., Faden, A.I., 2014b. Spinal cord injury causes brain inflammation associated with cognitive and affective changes: role of cell cycle pathways. *J. Neurosci.* 34, 10989–11006. <https://doi.org/10.1523/JNEUROSCI.5110-13.2014>.
- Young, W., 2002. Spinal cord contusion models. *Prog. Brain Res.* 137, 231–255. [https://doi.org/10.1016/s0079-6123\(02\)37019-5](https://doi.org/10.1016/s0079-6123(02)37019-5).
- Zeng, P.Y., Tsai, Y.H., Lee, C.L., Ma, Y.K., Kuo, T.H., 2023. Minimal influence of estrous cycle on studies of female mouse behaviors. *Front. Mol. Neurosci.* 16, 1146109. <https://doi.org/10.3389/fnmol.2023.1146109>.
- Zhao, W., Li, Q., Ma, Y., et al., 2021. Behaviors related to psychiatric disorders and pain perception in C57bl/6J mice during different phases of estrous cycle. *Front. Neurosci.* 15, 650793. <https://doi.org/10.3389/fnins.2021.650793>.
- Zimmermann, M., 1983. Ethical guidelines for investigations of experimental pain in conscious animals. *Pain* 16 (2), 109–110. [https://doi.org/10.1016/0304-3959\(83\)90201-4](https://doi.org/10.1016/0304-3959(83)90201-4).